

Nuclear Structure Studies with the ${}^7\text{Li}(e, e'p)$ Reaction

L. Lapikás,¹ J. Wesseling,¹ and R. B. Wiringa²

¹NIKHEF, P.O. Box 41882, 1009 DB Amsterdam, The Netherlands

²Physics Division, Argonne National Laboratory, Argonne, Illinois 60439

(Received 21 September 1998)

Experimental momentum distributions for the transitions to the ground state and first excited state of ${}^6\text{He}$ have been measured via the reaction ${}^7\text{Li}(e, e'p){}^6\text{He}$. They are compared to theoretical distributions calculated with variational Monte Carlo (VMC) wave functions which include strong state-dependent correlations in both ${}^7\text{Li}$ and ${}^6\text{He}$. These VMC calculations provide a parameter-free prediction that reproduces the measured data, including its normalization. The deduced spectroscopic factor for the two transitions is 0.58 ± 0.05 , in perfect agreement with the VMC value of 0.60. This is the first successful comparison of experiment and *ab initio* theory for spectroscopic factors in *p*-shell nuclei. [S0031-9007(99)09267-4]

PACS numbers: 21.10.Jx, 21.60.Ka, 25.30.Dh, 27.20.+n

In this Letter we present new experimental data on the reaction ${}^7\text{Li}(e, e'p){}^6\text{He}$ and compare the deduced momentum distributions with recent *ab initio* predictions from variational Monte Carlo (VMC) calculations. Some years ago, two of us (Lapikás and Wesseling) participated in electron scattering experiments to determine shell occupancies in the nuclei ${}^{30}\text{Si}$, ${}^{31}\text{P}$, and ${}^{32}\text{S}$ [1,2]. In the latter case, a Li_2S target was used, with resolution sufficient to separate the discrete transitions in the reaction ${}^{32}\text{S}(e, e'p){}^{31}\text{P}$ from those in the reaction ${}^7\text{Li}(e, e'p){}^6\text{He}$. However, the results for ${}^7\text{Li}$ were not published at the time. Independently, one of us (Wiringa) recently calculated the overlap wave function $\langle {}^6\text{He}|a(\mathbf{r})|{}^7\text{Li}\rangle$ as part of a general program of quantum Monte Carlo studies of the light *p*-shell nuclei [3,4]. These calculations use realistic two- and three-nucleon interactions fit to *NN* scattering data and few-body nuclear bound states, and produce fully correlated *A*-body wave functions. We have now found that using the VMC overlap as input to a Coulomb distorted wave impulse approximation (CDWIA) code results in excellent predictions of the observed momentum distributions and transition rms radii including the absolute normalization of the cross sections. This is the first successful comparison of experiment and *ab initio* theory for spectroscopic factors in *p*-shell nuclei.

The effect of including short-range and tensor correlations in the calculation of nuclear structure has been studied previously in detail for few-body systems. In particular, momentum distributions for the nuclei ${}^2\text{H}$ [5,6], ${}^3\text{He}$ [7], and ${}^4\text{He}$ [8,9], measured via the reaction $(e, e'p)$, have been compared to calculations (Faddeev [10] and VMC [11,12]) that include state-dependent correlations derived from bare nucleon-nucleon interactions. Experiments on complex ($A > 4$) nuclei have been performed [13] abundantly, but theoretical calculations (Green's function [14] and cluster VMC [15]) are more difficult, and have been limited to a few closed-shell nuclei; as discussed below, these usually overpredict the normalization of the cross sections. Typically, these data (consisting mainly of

knockout of valence protons) are analyzed by comparing to calculations based on mean-field theory (MFT) that do not include (short-range and other) correlations, and by identifying the required renormalization as the spectroscopic factor. The resulting factors [13,16] (about 60%–65% for nuclei ranging from $A = 6$ to 209) are usually interpreted as evidence for the presence of important correlations.

A quenching of this kind was predicted for infinite nuclear matter [17,18] but the extension of this result to finite nuclei is not straightforward due to the coupling to surface vibrations that affects the strength for transitions near the Fermi edge. For the nucleus ${}^{16}\text{O}$ the effect of both short- and long-range correlations was calculated with a Green's function method [14] resulting in a reduction of the strength to 0.76 of the MFT value. However, the inclusion of center-of-mass effects will probably increase this value to ~ 0.81 [15], which is still considerably larger than the observed [19] $1p$ strength (~ 0.6) at small excitation energies. It may be that ${}^{16}\text{O}$ is an exceptionally difficult case; more success has been gained with the larger nuclei ${}^{48}\text{Ca}$ and ${}^{90}\text{Zr}$ [20], although these calculations must use a *G*-matrix representation of the *NN* force, a step away from the bare interaction. In the present case, the VMC method uses the bare interactions to produce rather sophisticated six- and seven-body wave functions, including strong state-dependent correlations, which show the clustering expected in light *p*-shell nuclei.

The theoretical description of the reaction $(e, e'p)$ has been given in detail elsewhere [21]. In plane-wave impulse approximation (PWIA), the expression for the cross section reads

$$\frac{d\sigma}{dE_{e'} d\Omega_{e'} dT_p d\Omega_p} = K \sigma_{\text{ep}} S(E_m, \mathbf{p}_m), \quad (1)$$

where the spectral function $S(E_m, \mathbf{p}_m)$ denotes the probability to find a proton with separation energy and momentum (E_m, \mathbf{p}_m) in the nucleus. The quantity $K \sigma_{\text{ep}}$ is

the product of a phase space factor and the elementary off-shell electron-proton cross section [22] that describes the coupling of the virtual photon to the proton. In this paper we consider the transitions to the 0^+ ground state ($E_m = 9.97$ MeV) and 2^+ first excited state ($E_m = 11.77$ MeV) in ${}^6\text{He}$. Hence in Eq. (1) E_m has two discrete values, and we can obtain the momentum distribution $\rho(\mathbf{p}_m)$ for each transition by integrating $S(E_m, \mathbf{p}_m)$ over the appropriate peak in E_m . In PWIA the momentum distributions are related to the overlap wave function $\langle {}^6\text{He}|a(\mathbf{r})|{}^7\text{Li}\rangle$ via

$$\rho(\mathbf{p}_m) = \left| \int e^{i\mathbf{p}_m \cdot \mathbf{r}} \langle {}^6\text{He}|a(\mathbf{r})|{}^7\text{Li}\rangle d\mathbf{r} \right|^2. \quad (2)$$

For the overlap wave functions we take either the MFT or the VMC results, which are discussed below. In order to account for Coulomb distortion of the electron wave functions and for final-state interaction (FSI) between the outgoing proton and the residual ${}^6\text{He}$ nucleus we use a CDWIA procedure [23]. Here the FSI is treated via an optical-model potential, the parameters of which were taken from a 100 MeV proton scattering experiment on ${}^6\text{Li}$ [24]. For the extrapolation of these parameters to 90 MeV protons and ${}^6\text{He}$ we used Schwandt's [25] global parametrization for a large number of nuclei and energies. The uncertainty due to the treatment of the FSI was estimated by also extrapolating the optical-model parameters from proton scattering data at lower [26] and higher [27,28] energies. This yielded model uncertainties on the spectroscopic factors of 6% and on the deduced rms radii of the overlap wave functions of 2%.

In mean-field theory the overlap wave function $\langle {}^6\text{He}|a(\mathbf{r})|{}^7\text{Li}\rangle$ reduces to a single-particle wave function $\phi_\alpha(\mathbf{r})$ since it is the product of two Slater determinants. It is taken as the solution of the Schrödinger equation with a Woods-Saxon potential that reproduces the appropriate binding energy. The radius of the potential is chosen such that the calculated momentum distribution fits the experimental data. Based on the VMC calculations, which predict dominant $1p_{3/2}$ and $1p_{1/2}$ amplitudes for the two transitions, respectively, we choose a MFT $1p_{3/2}$ wave function for the $3/2^- \rightarrow 0^+$ ground-state transition and a $1p_{1/2}$ MFT wave function for the $3/2^- \rightarrow 2^+$ transition to the first excited state.

Quantum Monte Carlo calculations of the ground and low-lying excited states for six- and seven-body nuclei have been made [3] using a realistic Hamiltonian containing the Argonne v_{18} two-nucleon [29] and Urbana IX three-nucleon [30] potentials (AV18/UIX model). These calculations start with trial functions, $\Psi_V(J^\pi, T)$, constructed from products of two- and three-body correlation operators acting on a fully antisymmetrized set of one-body p -shell basis states that are LS coupled to the specified quantum numbers. Metropolis Monte Carlo integration [31] is used to evaluate $\langle \Psi_V | H | \Psi_V \rangle$ and diagonalize in the one-body p -shell basis, giving upper bounds to the energies of these states. The trial functions are then

used as input to the Green's function Monte Carlo (GFMC) algorithm, which projects out excited state contamination in the trial function by means of the Euclidean propagation $\Psi(\tau) = \exp[-(H - E_0)\tau]\Psi_V$. The GFMC results are believed to be within $\sim 1\%$ of the exact binding energy for the given Hamiltonian.

For the AV18/UIX model, the GFMC energy for the ${}^7\text{Li}$ ground state is $-37.4(3)$ MeV, where the number in parentheses is the statistical error due to the Monte Carlo energy evaluation. The ${}^6\text{He}(0^+)$ ground state is at $-27.6(1)$ MeV and the ${}^6\text{He}(2^+)$ excited state is at $-25.8(2)$ MeV. While these *ab initio* energies are about 5% above experiment (which we attribute to inadequacies of the AV18/UIX model) the relative excitations of $9.8(3)$ and $11.6(3)$ MeV are fairly close to experiment. The VMC energies are not as good, but the one- and two-body VMC and GFMC density distributions are very similar, giving us some confidence in using the Ψ_V to study reactions. Recent calculations using the equivalent Ψ_V for ${}^6\text{Li}$ gave a very satisfactory description of both elastic and inelastic electron scattering form factors [32]. For the present Letter, the $\langle {}^6\text{He}|a(\mathbf{r})|{}^7\text{Li}\rangle$ overlaps were calculated using the techniques of Refs. [11,12].

In Figs. 1 and 2 we compare the plane wave MFT and VMC wave functions in momentum space out to large momenta. In order to facilitate the comparison we have scaled the MFT overlap wave functions such that their normalization is identical to that of the VMC wave functions. For the ground-state transition (see Fig. 1) we observe that the MFT and VMC wave functions are practically identical up to $p_m = 400$ MeV/c, whereas above this momentum the

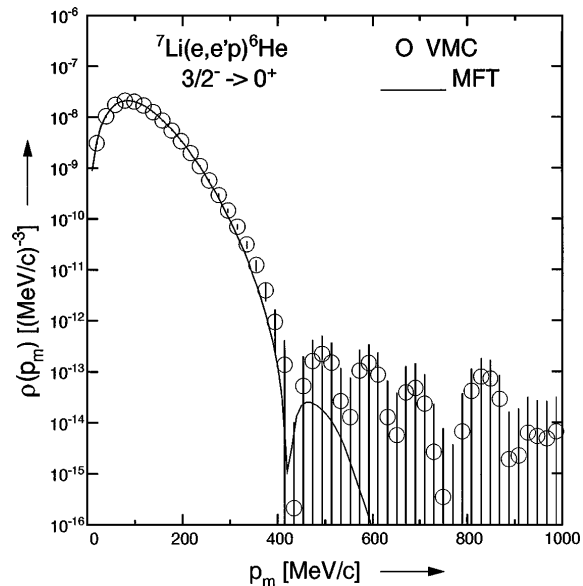


FIG. 1. Momentum distributions in PWIA for the ground-state overlap wave function $\langle {}^6\text{He}|a(\mathbf{r})|{}^7\text{Li}\rangle$ as calculated in MFT (solid curve) and in VMC (circles). The error bars on the VMC data denote the uncertainty due to Monte Carlo sampling. The normalization of the MFT wave function has been chosen identical to that of the VMC one.

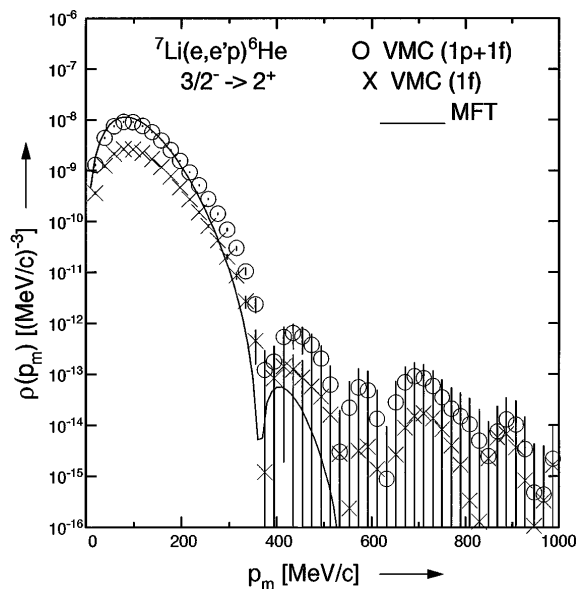


FIG. 2. Same as Fig. 1 but for the transition to the first excited state. The MFT wave function is pure $1p_{1/2}$, the total VMC wave function (circles) contains $1p$ and $1f$ (crosses) components.

VMC wave function is appreciably larger due to the inclusion of short-range and tensor correlations, which are absent in MFT. The transition to the first excited state contains both $1p$ and $1f$ components, as shown in Fig. 2. Here the deviation between the VMC and MFT wave function already starts at 250 MeV/c because in MFT the wave function is purely $1p_{1/2}$, whereas the VMC overlap contains four components ($1p_{1/2}$, $1p_{3/2}$, $1f_{5/2}$, $1f_{7/2}$). In addition to the effect of correlations, these extra components cause an appreciable enhancement of the VMC wave function at high momentum relative to the MFT wave function.

The experiment was performed with the 1% duty factor electron beam from the NIKHEF medium-energy accelerator and the high-resolution two-spectrometer setup in the EMIN end station [33]. The data were taken concurrently with those for the reaction $^{32}\text{S}(e, e'p)$ [1,2] for which purpose a self-supporting disk of Li_2S was used as a target (thickness roughly 25 mg/cm²). The target could withstand maximum average currents of 6 μA when rotated continuously. The target thickness was monitored via frequent measurements of elastic scattering. The measurements were carried out in parallel kinematics for an outgoing proton energy of 90 MeV. As a result we needed two incident energies (329.7 and 454.7 MeV) to cover the missing momentum range of -70 to 260 MeV/c. Since the beam was tuned in dispersion matching mode [34] we could achieve an E_m resolution of 180 keV (FWHM), sufficient to separate the discrete transitions from the two reactions.

The data analysis was performed in a standard way described in detail elsewhere [35]. From the measured cross sections we determined momentum distributions by integrating over the appropriate missing-energy peak

and by dividing out $K\sigma_{ep}$, for which we used the current-conserving expression σ_{ep}^{cc1} of de Forest [22]. The resulting experimental momentum distributions are shown in Fig. 3, where only the statistical errors are shown. The experimental systematic uncertainty on these data is 5%.

In the only earlier reported [36] study of the reaction $^7\text{Li}(e, e'p)^6\text{He}$ the missing-energy resolution of 7 MeV was insufficient to separate the two transitions presented in this Letter. However, when corrected for the presence of some unresolved $1s$ knockout strength and the difference in ejected proton energy, their momentum distribution, integrated over the region $E_m = 6$ –15 MeV, agrees within error bars with that for the sum of the two transitions studied here.

In order to compare the theoretical calculations with the data we carried out CDWIA calculations with the MFT and VMC wave functions as input. For the mean-field calculations we treated the normalization, i.e., the spectroscopic factor S , and the radius of the WS potential (that fixes the rms radius $\langle r^2 \rangle^{1/2}$ of the wave function) as free parameters to be determined from a least squares fit to the data. The resulting values are listed in Table I. The summed spectroscopic strength for $1p$ knockout is 0.58 ± 0.05 , where we have included the experimental systematic uncertainty and the uncertainty due to the choice of the optical potential. The observed reduction of the single-particle strength to 58% of the MFT value (which is unity for a single proton in the $1p$ shell) is in good agreement with the reduction found for a large number of other complex nuclei [13].

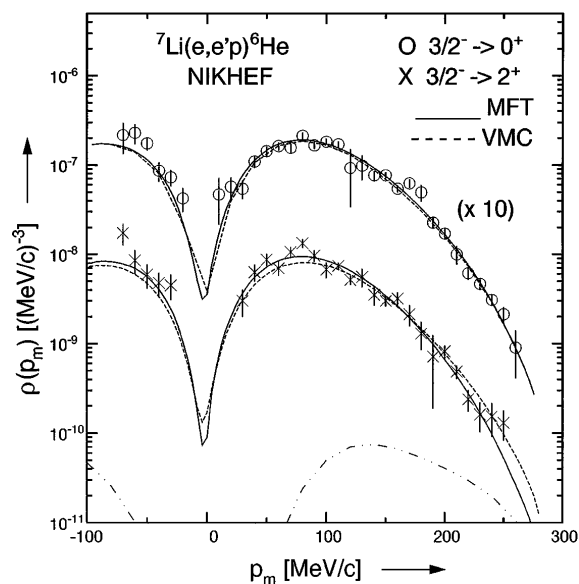


FIG. 3. Experimental momentum distributions for the transitions to the ground state (circles) and first excited state (crosses) in the reaction $^7\text{Li}(e, e'p)^6\text{He}$, compared to CDWIA calculations with MFT (solid) and VMC (dashed) wave functions. The dot-dot-dashed curve represents the $1f$ contribution to the full VMC curve for the 2^+ state. The error bars on the data are statistical only. For clarity data and curves for the ground-state transition have been scaled by 10.

TABLE I. Spectroscopic factors (S) and rms radii deduced in the present experiment for the transitions to the 0^+ and 2^+ states in ${}^6\text{He}$ (first row). The listed errors include statistical, systematic, and model uncertainties. The second (third) row presents the corresponding values for the VMC calculation with $1p$ ($1p + 1f$) wave function components.

Model	S	S	S	rms (fm)	rms (fm)
	0^+	2^+	$0^+ + 2^+$	0^+	2^+
Expt. ($1p$)	0.42(4)	0.16(2)	0.58(5)	3.17(6)	3.47(9)
VMC ($1p$)	0.41	0.18	0.59	3.16	3.14
VMC ($1p + 1f$)	0.41	0.19	0.60	3.16	3.16

Figure 3 also shows the calculated momentum distributions with the VMC wave functions, which are essentially parameter-free. The agreement with the data is very good as shown in Table I where the calculated spectroscopic factors with these wave functions are given. The summed strength (0.60) for both transitions agrees within error bars perfectly with the value 0.58 ± 0.05 deduced from the MFT analysis.

The VMC rms radius for the ground-state transition agrees with the value deduced from the MFT analysis, showing that the calculated VMC ground-state wave functions for ${}^6\text{He}$ and ${}^7\text{Li}$ have the correct shape. For the transition to the first excited state the rms radius of the VMC wave function is smaller than that found in the MFT analysis. This is caused by the different structure for both overlaps: the MFT wave function was assumed to be pure $1p_{1/2}$, whereas the VMC wave function contains $1p_{3/2}$, $1f_{5/2}$, and $1f_{7/2}$ components in addition. The contributions of the $1f$ components, which depend sensitively on the details of the nucleon-nucleon interaction employed, would show up in measurements at higher p_m and could thereby serve as a further accurate test of the VMC wave functions.

In summary, we conclude that for the first time structure calculations for a complex nucleus, based on a realistic nucleon-nucleon force, have been performed and compared to (new) experimental data for the reaction ${}^7\text{Li}(e, e'p)$. The calculated spectroscopic strength (0.60) explains the reduction of the strength to 0.58 ± 0.05 found in a MFT analysis of the data, while the calculated shape of the momentum distributions for $1p$ transitions nearly coincides with the experimental data. Thus we have confirmed the necessity of including full correlations in the nuclear wave functions.

We thank Dr. G. van der Steenhoven for a helpful discussion. This work is part of the research program of the Foundation for Fundamental Research of Matter (FOM), which is financially supported by the Netherlands' Organisation for Advancement of Pure Research (NWO). The work of R. B. W. is supported by the U.S. Department of Energy, Nuclear Physics Division, under Contract No. W-31-109-ENG-38.

[1] J. Wesseling *et al.*, Nucl. Phys. **A547**, 519 (1992).

- [2] J. Wesseling *et al.*, Phys. Rev. C **55**, 2773 (1997).
 [3] B. S. Pudliner *et al.*, Phys. Rev. C **56**, 1720 (1997).
 [4] R. B. Wiringa, Nucl. Phys. **A631**, 70c (1998).
 [5] K. I. Blomqvist *et al.*, Phys. Lett. B **424**, 33 (1998).
 [6] W.-J. Kasdorp *et al.*, Few Body Syst. **25**, 115 (1998).
 [7] C. Marchand *et al.*, Phys. Rev. Lett. **60**, 1703 (1988).
 [8] J. M. Le Goff *et al.*, Phys. Rev. C **50**, 2278 (1994).
 [9] J. J. van Leeuwe *et al.*, Phys. Rev. Lett. **80**, 2543 (1998).
 [10] J. Golak *et al.*, Phys. Rev. C **51**, 1638 (1995).
 [11] R. Schiavilla, V. R. Pandharipande, and R. B. Wiringa, Nucl. Phys. **A449**, 219 (1986).
 [12] J. L. Forest *et al.*, Phys. Rev. C **54**, 646 (1996).
 [13] L. Lapidás, Nucl. Phys. **A553**, 297c (1993).
 [14] W. J. W. Geurts *et al.*, Phys. Rev. C **53**, 2207 (1996).
 [15] D. Van Neck *et al.*, Phys. Rev. C **57**, 2308 (1998).
 [16] V. R. Pandharipande, I. Sick, and P. K. A. de Witt Huberts, Rev. Mod. Phys. **69**, 981 (1997).
 [17] O. Benhar, A. Fabrocini, and S. Fantoni, Nucl. Phys. **A505**, 267 (1989).
 [18] A. Ramos, A. Polls, and W. H. Dickhoff, Nucl. Phys. **A503**, 1 (1989).
 [19] M. Leuschner *et al.*, Phys. Rev. C **49**, 955 (1994).
 [20] G. A. Rijdsdijk *et al.*, Phys. Rev. C **53**, 201 (1996); Nucl. Phys. **A550**, 159 (1992).
 [21] A. E. L. Dieperink and T. de Forest, Jr., Annu. Rev. Nucl. Sci. **25**, 1 (1975).
 [22] T. de Forest, Jr., Nucl. Phys. **A392**, 232 (1983).
 [23] C. Giusti and F. Pacati, Nucl. Phys. **A485**, 461 (1988).
 [24] T. Y. Li and S. K. Mark, Can. J. Phys. **46**, 2645 (1968).
 [25] P. Schwandt *et al.*, Phys. Rev. C **26**, 55 (1982).
 [26] K. H. Bray *et al.*, Nucl. Phys. **A189**, 35 (1972).
 [27] R. S. Henderson *et al.*, Nucl. Phys. **A372**, 117 (1981).
 [28] G. L. Moake and P. T. Debevec, Phys. Rev. C **21**, 25 (1980).
 [29] R. B. Wiringa, V. G. J. Stoks, and R. Schiavilla, Phys. Rev. C **51**, 38 (1995).
 [30] B. S. Pudliner *et al.*, Phys. Rev. Lett. **74**, 4396 (1995).
 [31] R. B. Wiringa, Phys. Rev. C **43**, 1585 (1991).
 [32] R. B. Wiringa and R. Schiavilla, Phys. Rev. Lett. **81**, 4317 (1998).
 [33] C. de Vries *et al.*, Nucl. Instrum. Methods Phys. Res., Sect. A **223**, 1 (1984).
 [34] P. K. A. de Witt Huberts and L. Lapidás, in *Proceedings of the Workshop on the use of Electron Rings for Nuclear Physics Research in the Intermediate Energy Region, Lund, 1982* (University of Lund, Lund, 1983) Vol. 1, p. 60.
 [35] J. W. A. den Herder *et al.*, Nucl. Phys. **A490**, 507 (1988).
 [36] K. Nakamura *et al.*, Nucl. Phys. **A296**, 431 (1978).